

External structure of a prototype Effervescent Diesel Injector-produced spray

Z. Liu, P.E. Sojka and J.P. Gore

Maurice J. Zucrow Laboratories/School of Mechanical Engineering
500 Allison Road
Purdue University
West Lafayette, IN 47907-2014
Email: Sojka@ecn.purdue.edu

A study was conducted to examine the external spray structure of a prototype Effervescent Diesel Injector (EDI) spray. The external spray structure was described by spray patternation, cone half-angle, and entrainment. The prototype EDI was configured with two different exit orifice sizes (0.18 and 0.33 mm diameters) and three needle lifts (0.029, 0.076, and 0.32 mm nominal) and was operated at injection pressures from 10.3 to 34.5 MPa and gas-liquid-ratios (GLRs) from 1 to 10%. A Gaussian curve fit showed that the EDI spray patternation data exhibit the same functional relationship as that of a single-phase turbulent jet. Cone half-angles calculated from patternation measurements were found to increase with injection pressure and exit orifice diameter. The entrainment numbers were: 0.17 ± 0.033 for the 0.18 mm orifice (insensitive to GLR) and 0.17 ± 0.045 (sensitive to GLR). Overall, the external spray characteristics of the larger orifice (0.33 mm diameter) exhibited a dependence on GLR while those for the smaller orifice (0.18 mm diameter) did not.

1. Introduction

Current Diesel injectors are designed with small exit orifices and operate at high injection pressures to meet emissions standards while maintaining efficiency. These requirements drive up the cost of engine manufacturing and maintenance. The advantages of effervescent atomization may be an answer to reducing costs and simplifying manufacturing. The only drawback of effervescent atomization is that it requires an onboard-pressurized gas supply.

Effervescent atomization was developed by Lefebvre [1] and coworkers and has been proposed for many potential applications. Wade *et al.* [2] were the first to use effervescent atomization for Diesel injection. Their work showed proof-of-concept, and that: (i) cone angle increases with GLR, possibly due to the increased energy from the expanding gas; (ii) cone angle increases with injection pressure at high injection pressures (12.6 to 36.5 MPa); (iii) that cone angle increases somewhat with an increase in orifice diameter.. Satapathy *et*

al. [3] studied the effect of ambient density on EDI performance and found it had negligible effect on mean drop size. Sovani [4] designed an optically accessible EDI and investigated how internal flow structure affected spray characteristics. Sovani *et al.* [5] were also the first to measure the drop size of the prototype EDI. Their results demonstrated that EDIs can be packaged in the same hardware used for conventional Diesel injectors.

Cone angle and patternation are not the only external spray quantities of interest. Entrainment is also important since it has a direct bearing on local equivalence ratio. Bush and Sojka [6] and Sutherland *et al.* [7] measured entrainment for effervescent atomizers. Both found that entrainment number is influenced by GLR. Bush and Sojka's [6] study reported that entrainment varies with atomizer geometry and liquid properties. They attributed the dependence on atomizer geometry (i.e. orifice diameter) to low Reynolds number values and the inherent unsteadiness of the spray. Sutherland *et al.* [7] found no dependence of entrainment on either atomizer geometry or liquid properties. How prototype EDI entrainment scales with atomizer geometry is therefore in question so its study was included in this investigation.

In summary, the purpose of this study is to determine the external EDI spray field by establishing its boundary via cone angle data and then providing patternation data to find the liquid mass distribution throughout this region. Local equivalence ratio can then be derived from the liquid mass distribution and corresponding entrainment data, also reported here.

2. Experimental apparatus

The experimental apparatus consist of the prototype effervescent Diesel injector (EDI), its associated gas and liquid delivery systems, an optical patternator for patternation and cone angle measurements, a momentum rate probe, and an entrainment device.

The prototype EDI is an effervescent atomizer fitted inside a conventional Diesel injector body. It has a closed geometry needle, allowing the effect of needle lift on injector performance to be studied by interchanging needles. Nominal needle lifts of 0.029, 0.076 and 0.32 mm were used for both the 0.18 and 0.33 mm diameter needles.

The prototype EDI operates in steady-state mode and has only one down-firing orifice since it must run continuously and spray in the downward axial direction to take patternation and entrainment data.

Two types of fluids were used. Rock Valley Oil and Chemical Company's VISCOR 1487AW/2 SAE J967D ($\rho=796 \text{ kg/m}^3$, $\mu=2.8 \text{ mPa-s}$, $\sigma=0.028 \text{ N/m}$) was used for high pressure tests while a 41:59 mass ratio mixture of The CoolerTM and distilled water ($\rho=1015 \text{ kg/m}^3$, $\mu=2.7 \text{ mPa-s}$, $\sigma=0.026 \text{ N/m}$) was used for low pressure tests.

The optical patternator developed by Ullom and Sojka [8] was used to study how spray cone angle and radial mass distribution depend on injection pressure, GLR, and axial distance from the EDI tip. The EDI sprays through a laser sheet and an array detector compares the light intensity transmitted through the spray to that when no spray is present. A data acquisition program calculates and plots a pattern value for each detector pixel. The spray edge is arbitrarily defined as the point of 97% transmission. This produces a consistent and quantitative definition for the spray boundary. Once the downstream axial distance from the exit orifice is determined, the spray cone angle is calculated from geometry. Patternator and cone angle uncertainties are estimated to be $\pm 0.4\%$ and $\pm 5\%$, respectively.

The momentum rate probe was developed by Bush *et al.* [9] and modified by Panchagnula and Sojka [10]. It measures the axial momentum rate of the spray by

redirecting it to the radial direction using a deflector cone hinged on a base plate with load cell. The load cell cone measures the force required to turn the spray. Uncertainty is estimated to be $\pm 1\%$.

Spray entrainment was measured using the instrument designed by Bush [11]; it is based on the Ricou and Spalding [12] device. When using this instrument, the injector is placed inside a double-walled cylindrical housing. Gas entrained into the spray must flow through a concentric porous cylinder that serves as the cylindrical housing inner wall. This ensures the entrained gas enters the spray with a uniform velocity profile. The position of the injector with respect to the cylinder exit plane can be adjusted, which changes the normalized axial distance along the spray (x/d) at which entrainment is measured. A differential pressure transducer is used to measure pressure drop between the inside and the outside of the housing. When this pressure drop reaches zero, the flow rate of the entrained air is assumed to equal that of the spray when it is located in an infinite environment. Uncertainty is estimated at $\pm 30\%$. This high value is due to the limited resolution of the micromanometer used to measure pressure drop across the entrainment device [11].

3. Results and discussion

Patteration, cone half-angle, momentum rate, and entrainment measurements were obtained for injection pressures from 10.3 to 34.5 MPa, gas-liquid ratios by mass (GLRs) between 1 and 10%, and axial distances of 10 to 100 mm.

3.1 Patteration

Patteration data were obtained in the form of pattern value as a function of patternator pixel number. The patteration plot shows drop area along a cross-section of the spray.

Fig. 1 is a typical patteration plot. Many such plots are available, but aren't shown here to conserve space; general trends are noted and quantitative results summarized.

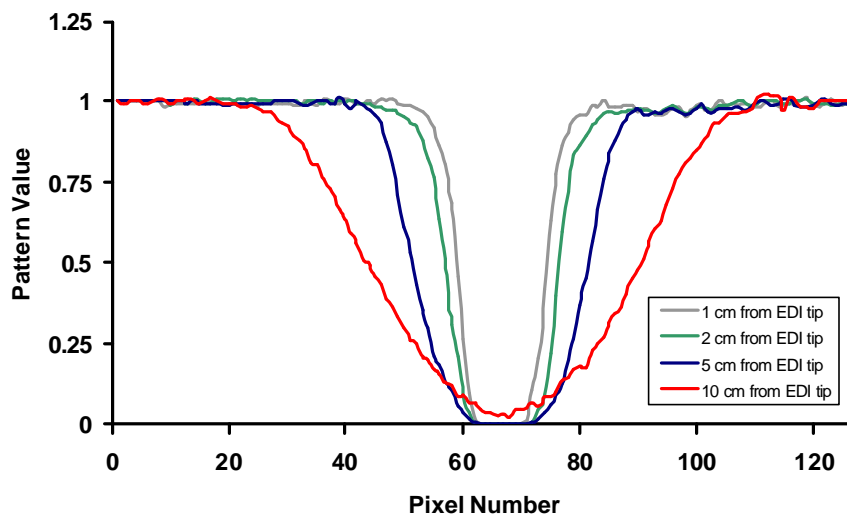


Fig. 1. Typical patteration for a prototype EDI spray at four axial distances, 0.33 mm diameter exit orifice, 0.030 mm needle lift, operating at 10.3 MPa injection pressure and 1% GLR.

Overall, the patterning plots indicate that the liquid mass flux is maximum at the center of the spray and decreases radially outward. As expected, the peak of the patterning curve decreases and its width increases with increasing distance from the EDI tip.

Comparison of patterning value versus pixel number plots shows spray width increases with orifice size, due to the increased volumetric flow rate from the larger orifice, but neither GLR nor needle lift variation has any significant impact on patterning. However, spray drop concentration becomes denser as injection pressure increases, which is expected. Lastly, the shape of the patterning curve resembles a Gaussian distribution.

Information contained in the large number of patterning plots was consolidated by performing a Gaussian curve fit to the data. Only 0.18 mm exit orifice diameter 10.3 MPa injection pressure results were used because only that data had patterning values greater than 0 (i.e., unsaturated) for all four axial locations considered. Note that some patterning data taken at 20.7 and 34.5 MPa were curve fitted and it was found that σ increased with injection pressure. However, there were not enough data at all axial locations for the higher pressures to be included here.

The relationship between pattern value and pixel number was described by $P = 1 - Ae^{-\frac{(r-r_0)^2}{2\sigma^2}}$ where P is the pattern value, A is the amplitude (pattern value at the centerline pixel), r is the pixel number, r_0 is the centerline pixel number (found using the method described by Ullom and Sojka [8]), and σ is the full width at half maximum, found by back-calculating it from the pattern value at each corresponding pixel number and taking the average over the entire curve. Fig. 2 shows a curve fit for one patterning measurement.

The curve fit results were used to study the effect of GLR, needle lift, and axial distance on A and σ . A linear relationship was found between σ and axial distance, as seen in Fig. 3 for three needle lifts and four GLRs. Uncertainty bars are ± 1 standard deviation of the data.

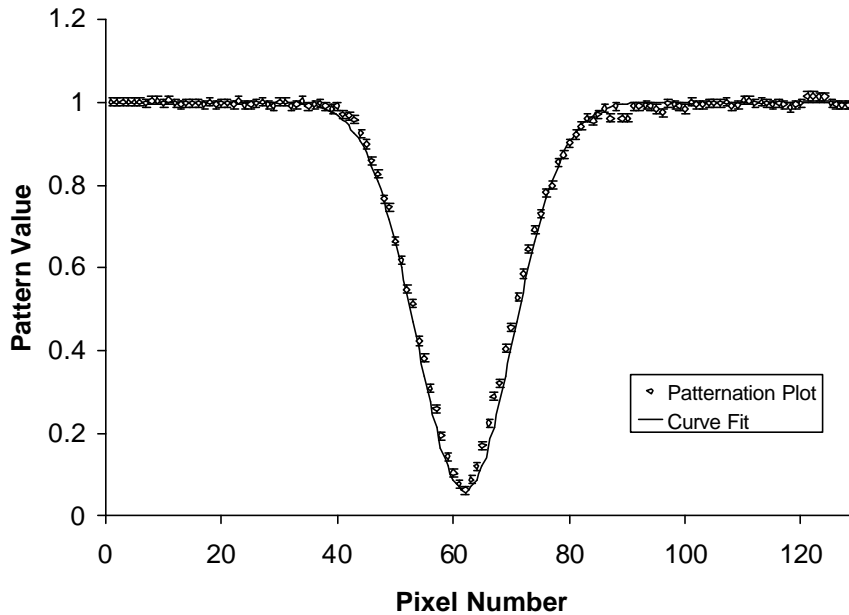


Fig. 2. Gaussian curve fit of patterning for 0.18 mm diameter exit orifice, 0.025 mm needle lift at 10.3 MPa injection pressure, 1% GLR, and 50 mm axial distance.

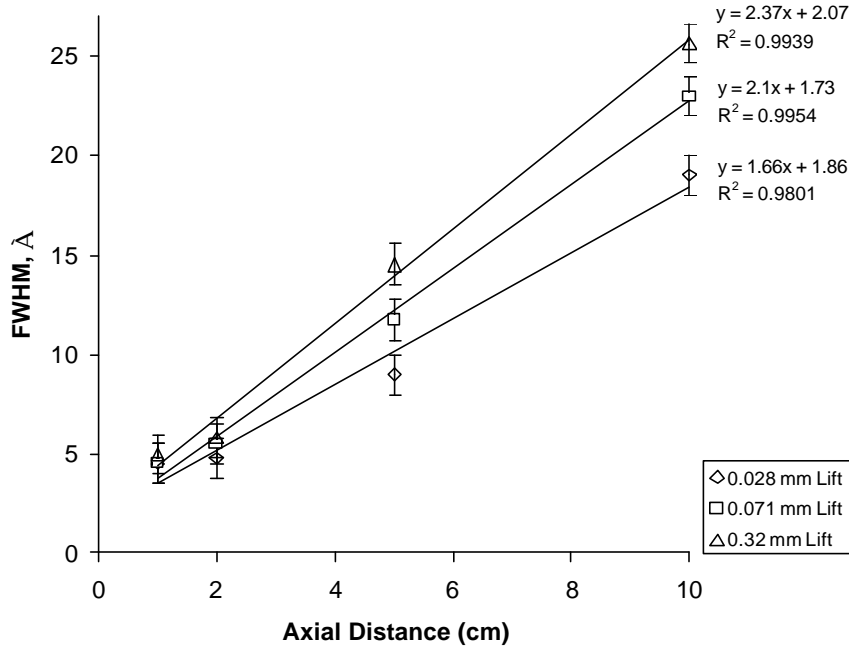


Fig.3. Typical full width at half maximum versus axial distance for an 0.18 mm diameter exit orifice operating at 10.3 MPa injection pressure, three needle lifts, and a GLR of 1%.

Fig. 3 demonstrates that σ increases monotonically with axial distance while all other parameters are held constant, regardless of needle lift and GLR. Furthermore, r^2 values are above 0.98 for all the operating conditions that could be curve fitted. Fig. 3 also shows σ increases slightly with needle lift, although many of the data points lie within each other's experimental uncertainty. Because the majority of the data show no dependence of σ on needle lift no quantitative conclusion is warranted. Finally, comparison of σ versus axial distance data for various GLRs showed no dependence of σ on GLR.

Amplitude describes the concentration of droplets in the spray via droplet area. A linear increase in amplitude with increasing inverse axial distance was observed. Typical results presented in Fig. 4 also show an inverse relationship between amplitude and needle lift. The dependence of σ on axial distance and amplitude on inverse axial distance is also characteristic of the behavior of an axisymmetric single-phase turbulent round jet.

3.2 Cone Angle

Spray cone half-angles were calculated from the patterning data, and are reported as cone half-angles. As expected, cone half-angle is a maximum near the exit orifice and decreases as the spray travels downstream. Two representative plots of cone half-angle versus GLR for two different orifice sizes and identical operating conditions are presented in Fig. 5.

As Fig. 5 shows, cone half-angle for the 0.18 mm orifice is not dependent on GLR, nor is it influenced by needle lift. The independence of cone half-angle with respect to GLR is consistent with the patterning curve fit findings reported in the previous section, but contradicts previous studies by Wade *et al.* [2] and Sovani *et al.* [5]. However, data presented by Wade *et al.* [2] show that cone half-angle only increases at GLRs above 10%. Below 10% GLR, both sets of data show cone half-angle is independent of GLR.

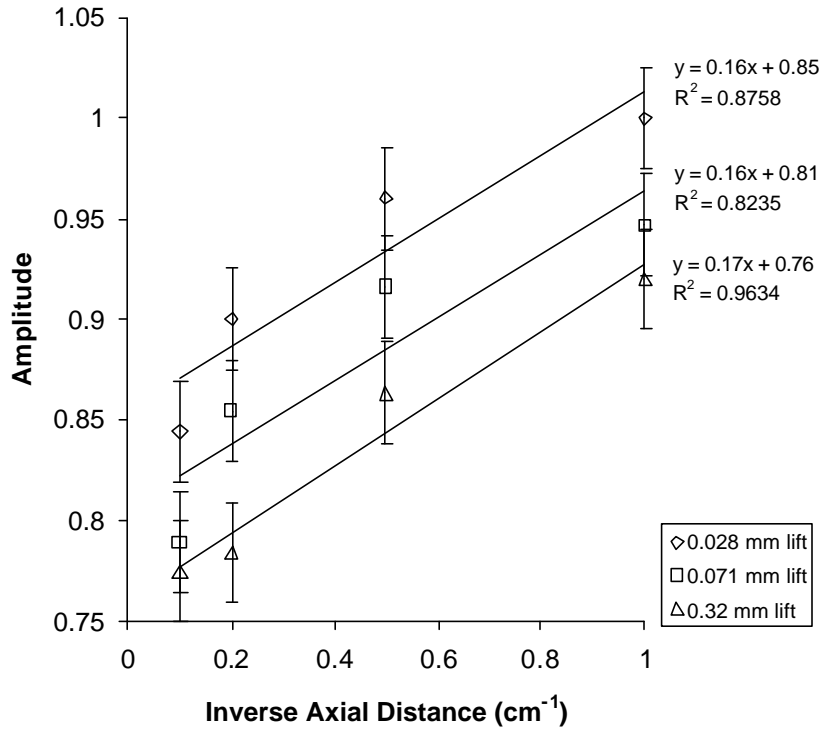


Fig. 4. Amplitude versus inverse axial distance at an injection pressure of 10.3 MPa with an 0.18 mm diameter exit orifice, three needle lifts, and GLR of 1%.

An examination of cone half-angle versus injection pressure data also shows that cone half-angles increased by as much as 25% from 10.3 to 34.5 MPa. Wade *et al.* [2] and Sovani *et al.* [5] both observed a similar trend. Note that the cone half-angle values shown here do not agree with the values reported by Wade *et al.* [2], who measured cone half-angles with the 0.18 mm orifice experimental EDI. This discrepancy may be due to the fact that different measurement methods were used.

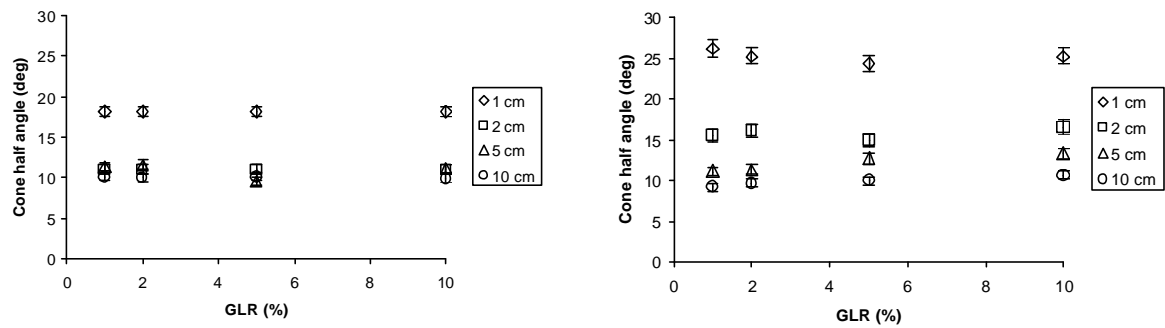


Fig. 5. Cone half-angle versus GLR at 20.7 MPa injection pressure with a 0.028 mm nominal needle lift at four axial distances: (left) 0.18 mm exit orifice, (right) 0.33 mm exit orifice.

Cone half-angle data for the 0.33 mm orifice show different trends between measurements taken near the exit orifice (< 2 cm) and those obtained further downstream (> 5 cm). Cone half-angle remains constant near the exit orifice. Further downstream cone half-angle increases marginally with GLR, with the magnitude of increase for most cases within experimental uncertainty. Thus, no quantitative relationship is warranted.

Cone half-angle increases with injection pressure, which agrees with results from Wade *et al.* [2] and Sovani *et al.* [5]. Like the 0.18 mm diameter exit orifice data, cone half-angle data for the 0.33 mm diameter exit orifice show no direct dependence on needle lift.

The effect of orifice diameter on spray cone half-angle could not be studied in detail because only two exit orifice diameters were used. However, cone half-angle data at 10.3 and 20.7 MPa showed the larger exit orifice produced sprays with wider cone half-angles. In contrast, at 34.5 MPa, cone half-angles from the two exit orifices were very similar.

3.3 Entrainment Number

Entrainment data collected using the entrainment device and momentum rate data collected using the momentum rate probe were used to calculate entrainment numbers. Data could not be taken at 10.3 MPa injection pressure for the 0.18 mm diameter exit orifice or at 34.5 MPa injection pressure for the 0.33 mm diameter exit orifice due to gas supply system limitations.

Entrainment number results for both orifice sizes are presented in Fig. 6. Note that the entrainment number for the smaller orifice size does not follow previous trends: it remains constant over the entire GLR range. Momentum rate was also found to be constant over the entire GLR range for the 0.18 mm orifice. No reason could be found for these observations.

Figure 7 also includes entrainment numbers for the 0.33 mm diameter exit orifice data. Entrainment number initially increases with GLR then reaches an asymptotic value at high GLR, as has been previously observed by Bush and Sojka [6] and Sutherland *et al.* [7].

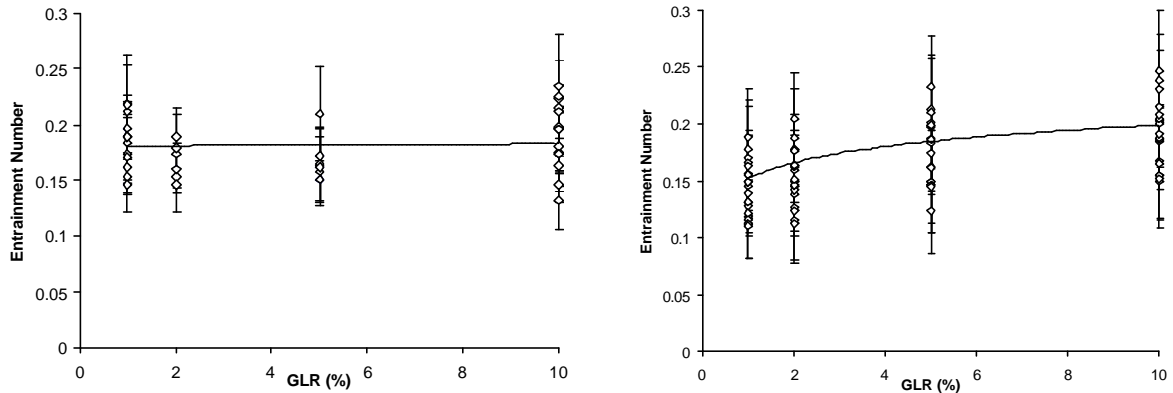


Fig. 6. Entrainment number versus GLR for: (left) 0.18 mm diameter exit orifice and (right) 0.33 mm diameter exit orifice at all operating conditions.

A comparison between large and small exit orifice diameter shows that the entrainment number is at most weakly dependent on orifice diameter. The entrainment number for the 0.18 mm orifice is 0.17 ± 0.033 and for the 0.33 mm orifice is 0.17 ± 0.045 . This value falls between the numbers reported by Ricou and Spalding [12] and Sutherland *et al.* [7]. The independence of entrainment number on orifice size contradicts findings by Bush and Sojka [6], who reported that entrainment number increases with orifice diameter. A constant entrainment number may indicate that the prototype EDI spray behaves as a gas jet.

4. Summary and conclusions

The external spray structure of a prototype Effervescent Diesel Injector was studied, with results reported as spray patterning, cone half-angle, momentum rate, and entrainment for operation at a wide range of injection pressures (10.3 to 34.5 MPa) and GLRs (1 to 10%).

Two different exit orifice diameters (0.18 to 0.33 mm) and three needle lifts (0.028 to 0.33 mm) were used. The injector configuration and test parameters are unique to this study.

Experimental results showed that the two exit orifices produced contrasting spray characteristics. While the 0.33 mm diameter exit orifice external spray structure followed trends found in previous studies, the 0.18 mm diameter exit orifice data did not. Previous studies have all reported that cone angle, momentum rate, and entrainment number increased with GLR.

An optical patternator was used to measure spray patternation and cone half-angle. A Gaussian curve fit was performed on the patternation data. The results showed that spray width was independent of GLR, but increased linearly with axial distance. Spray width also increased with orifice size and injection pressure, and amplitude was independent of GLR, but proportional to inverse axial distance and inversely proportional to needle lift.

Cone half-angle data showed no significant dependence on GLR. Overall, cone half-angle increased with injection pressure, but remained constant with changes in needle lift. The larger diameter exit orifice produced the widest cone half-angle.

Entrainment number results showed that the 0.33 mm diameter exit orifice data increased with GLR until an asymptotic value (0.17 ± 0.045) is reached at 10% GLR. On the other hand, entrainment number for the 0.18 mm diameter exit orifice was constant at 0.17 ± 0.033 irrespective of GLR.

The following conclusions are drawn from the results of this study:

1. The prototype EDI patternation has the same functional form as that of an axisymmetric single-phase turbulent jet.
2. Sprays produced by the 0.18 mm diameter exit orifice are not affected by variations in GLR, while sprays produced by the 0.33 mm diameter exit orifice do vary with GLR.
3. The entrainment number of the prototype EDI is independent of atomizer geometry and can be approximated as 0.17 ± 0.045 .

References

- [1] Lefebvre AH 1989 *Atomization and sprays* (Hemisphere: Washington, DC)
- [2] Wade RA, Weerts JM, Sojka PE, Gore JP and Eckerle WA 1999 *Atom. Sprays* **9** 651-67
- [3] Satapathy MR, Sovani SD, Sojka PE, Gore JP, Eckerle WA and Crofts JD 2000 *Atom Sprays* in revision
- [4] Sovani SD 2001 Ph.D. Thesis Purdue University
- [5] Sovani SD, Chou E, Sojka PE, Gore JP, Eckerle WA and Crofts JD 2001 *Fuel* **80** 427-435
- [6] Bush SG and Sojka PE 2003 *Atom. Sprays*
- [7] Sutherland JJ, Sojka PE and Plesniak MW 1997 *Int'l J. Multiphase Flow* **23** 865-884
- [8] Ullom MJ and Sojka PE 2001 *Rev. Sci. Instr.* **72** 2472-77
- [9] Bush SG, Bennett JB, Sojka PE, Panchagnula MV and Plesniak MW 1996 *Rev. Sci. Instr.* **67** 1878-85
- [10] Panchagnula MV, Sojka PE 1999 *Fuel* **78** 729-41
- [11] Bush, SG 1994 M.S.M.E. Thesis, Purdue University
- [12] Ricou FP and Spalding DB 1961 *J Fluid Mechanics* **11** 21-32